

Stabilization of Excited State Using Through-Space Interaction between Independent π -Systems Mediated by a *peri*-Substituted Hydroxy Group in 1-Arylnaphthalenes: Unexpected Blue Emission of 1,3,5-Tris(*peri*-hydroxynaphthyl)benzene

Hideto Nakajima,¹ Makoto Yasuda,^{*1,2} Kenji Shimizu,¹ Naomi Toyoshima,¹ Yasunori Tsukahara,³ Takao Kobayashi,⁴ Shinichiro Nakamura,⁴ Kouji Chiba,⁵ and Akio Baba^{*1}

¹Department of Applied Chemistry, Graduate School of Engineering, Osaka University, 2-1 Yamadaoka, Suita, Osaka 565-0871

²Center for Atomic and Molecular Technologies, Graduate School of Engineering, Osaka University, 2-1 Yamadaoka, Suita, Osaka 565-0871

³Graduate School of Engineering, Osaka University, 2-1 Yamadaoka, Suita, Osaka 565-0871

⁴Mitsubishi Chemical Group, Science and Technology Research Center, Inc., 1000 Kamoshida-cho, Aoba-ku, Yokohama 227-8502

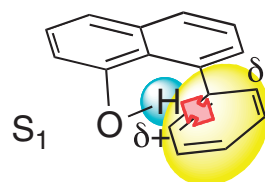
⁵Science and Technology Division, Ryoka Systems Inc., 1-28-38 Shinkawa, Chuo-ku, Tokyo 104-0033

Received May 13, 2011; E-mail: yasuda@chem.eng.osaka-u.ac.jp, baba@chem.eng.osaka-u.ac.jp

The control of photoluminescence wavelength is important for the design of emitting materials, and compounds bearing aryl–aryl bonds are considered to be useful candidates for the synthesis of these materials. However, the biaryl system lacks an efficient linkage of independent conjugated moieties because of a structure that, rather than planar, is made up of almost perpendicular dihedral angles due to steric effect. In this paper, we report a novel method to link independent π -systems in biaryl compounds. The oxy-substituents at the *peri*-position in 1-arylnaphthalene systems, which are biaryl compounds, showed interesting and unexpected photophysical properties of a bathochromic shift of emission. In particular, *peri*-OH-substituted arylnaphthalenes showed a large bathochromic shift that was induced by polarization based on intramolecular OH–aryl interaction. Quantum chemical (TDDFT) calculations accurately reproduced the large bathochromic shifts of *peri*-OH-substituted arylnaphthalenes. The through-space interaction between the *peri*-substituted OH and aryl groups generated an unexpected extended conjugation system. The substituting position of OH in 1-arylnaphthalenes is quite critical, because the hydroxy group mediates the independent π -systems to expand conjugation. Based on this concept, 1,3,5-tris(*peri*-hydroxynaphthyl)benzene had characteristic photophysical properties, giving an unexpected blue emission.

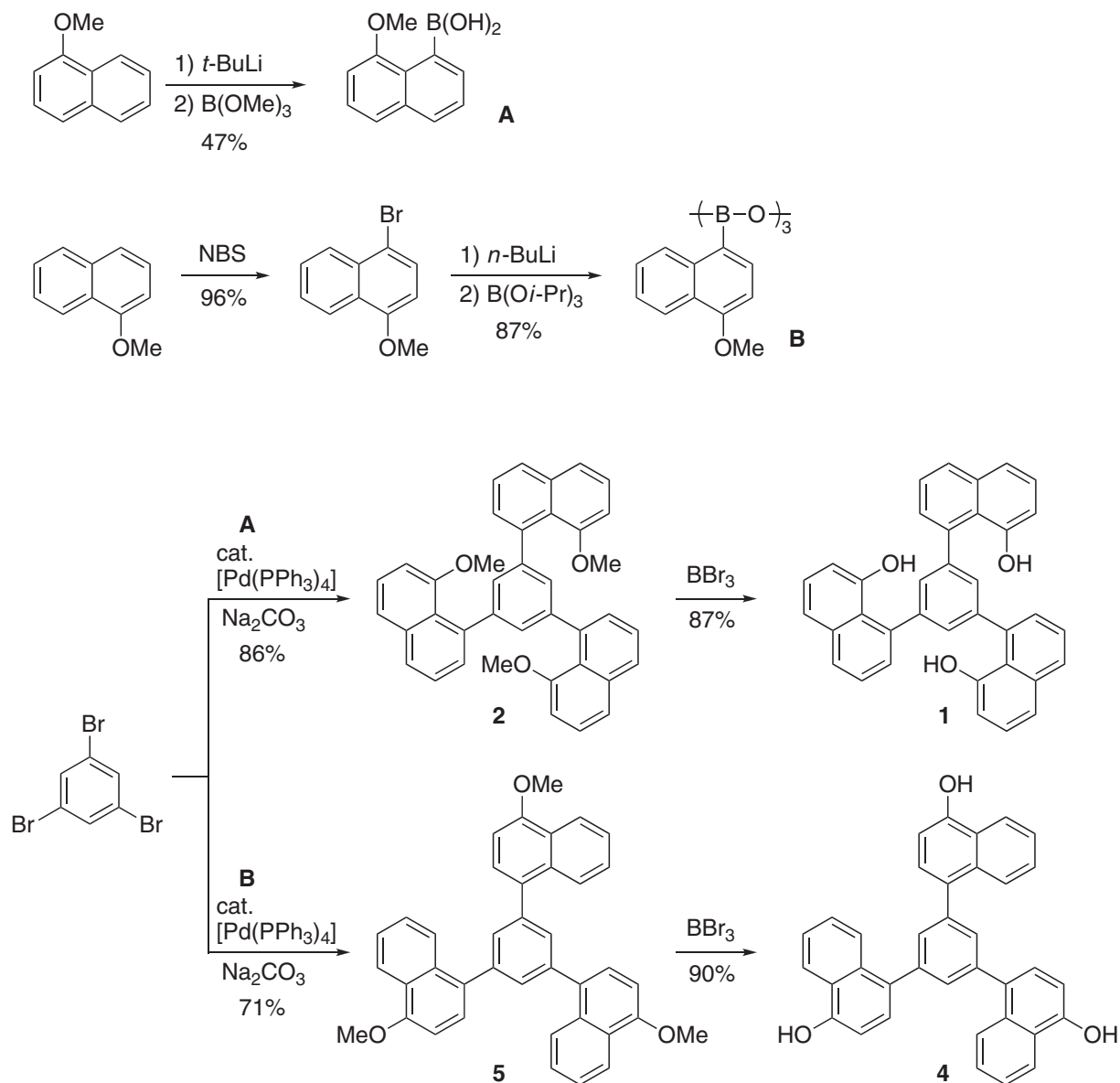
Control of photoluminescence wavelength is undoubtedly important for emitting materials. For this purpose, organic compounds are prepared based on π -conjugation systems with numerous types of structures and substituents. Conjugation in organic molecules can be designed employing synthetic chemistry, and various types of extended conjugation systems have been developed to bind independent conjugation systems through covalent bonds.¹ One of the most effective protocols is aryl–aryl coupling to expand π -systems.² Although a planar structure of π -systems could accomplish efficient conjugation, geometry around the aryl–aryl covalent bond usually does not show a planar structure, owing to the steric factor.³ Deviation from the planar structure decreases the effectiveness of the extension of conjugation systems. It often causes limitations in designing conjugated molecules. In this context, a methodology to link different π -systems that cannot be placed in a planar sphere would supply new strategies to design emitting materials. We herein report a novel “through-space” protocol

for stabilization of the excited state using a hydroxy group that mediates independent π -systems (Scheme 1). This “through-space” effect is more effective in the excited state than in the ground state, so a large Stokes shift is observed. Based on the proposed concept, an unexpected blue emission was realized by a tris(*peri*-hydroxynaphthyl)benzene system.



Stabilization by electrostatic interaction

Scheme 1. Through-space interaction of a biaryl compound in the S_1 state.



Scheme 2. Synthesis of tris(hydroxynaphthyl)benzenes.

Results and Discussion

Synthesis and Characterization of Tris(hydroxynaphthyl)benzenes and Their Derivatives. 1,3,5-Tris(8-hydroxy-1-naphthyl)benzene (**1**) was prepared from its methoxy-protected form **2**, which was formed by Suzuki–Miyaura coupling^{4,5} between 1,3,5-tribromobenzene and the boric acid **A**,⁶ as shown in Scheme 2. Regioisomers of **4** and **5**, bearing OH and OMe groups, respectively, on the *para*-positions, were also prepared in a similar manner using boric acid derivative **B**.

NMR study was employed using tris(hydroxynaphthyl)benzenes in DMSO-*d*₆.⁷ The ¹H NMR spectrum of **1** at room temperature (22 °C) showed one conformer that had a conformationally rigid structure bearing two of three OH groups in naphthyl groups on above the plane of a central benzene ring, and another OH group placed below the plane (OH direction; up–up–down); two types of signals, corresponding to hydroxy protons, were observed with a 2:1 integration ratio (see

Supporting Information).⁸ At a higher temperature (70 °C), OH moieties of compound **1** showed a single broad signal caused by fast equilibrium of the conformers. Compound **2**, with methoxy groups, showed a spectrum of mixtures of the two conformers (OMe direction; up–up–up and up–up–down) in a range from –60 °C to rt.⁹ A broad signal caused by fast equilibrium was observed at 60 °C. On the other hand, *para*-isomers **4** and **5** showed only one set of signals in ¹H NMR because of fast equilibrium based on a facile aryl–aryl bond rotation, even at room temperature. These observations suggest that, compared with the *para*-form, the *peri*-substituent led to a higher energy barrier for aryl–aryl bond rotation, and the *peri*-OH-substituted compound **1** exists mainly as one conformer with an up–up–down form at room temperature.

The solid-state structure of **1** was analyzed by X-ray crystallography, and the ORTEP drawing is shown in Figure 1. The structure showed an up–up–down conformation. Its geometry was the same in the solution state at room temper-

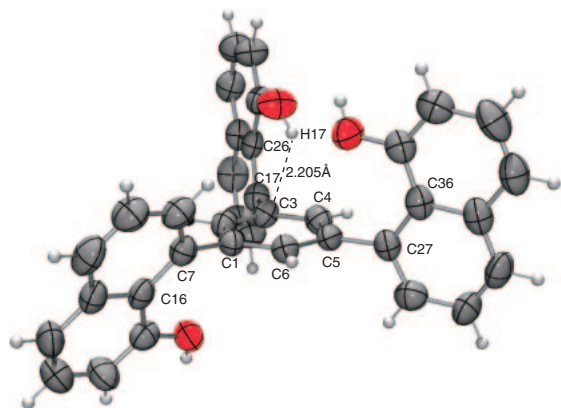


Figure 1. ORTEP drawing of **1**. Selected torsion angles and distance: C(6)–C(5)–C(27)–C(36) 89.10°, C(4)–C(3)–C(17)–C(26) 89.53°, C(6)–C(1)–C(7)–C(16) 69.21°, H(17)–C(3) 2.205 Å.

Table 1. Photophysical Data of Trinaphthylbenzene Derivatives

Compound	Absorption		Emission	
	λ_{\max}/nm	$\epsilon/10^4 \text{M}^{-1} \text{cm}^{-1}$	$\lambda_{\max}(\lambda_{\text{ex}})/\text{nm}$	Φ
1	320	2.69	446 (334)	0.01
2	307	2.70	382 (306)	0.04
3	296	3.91	360 (298)	0.22
4	316	2.77	392 (320)	0.01
5	309	3.93	376 (316)	0.18
6	299	0.579	366 (300)	0.07
7	295	0.717	340 (296)	0.38
8	278	0.608	336 (278)	0.31

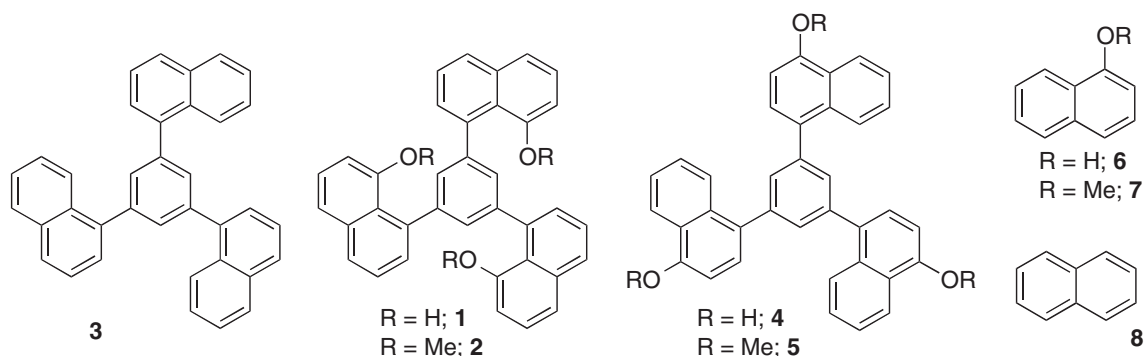


Chart 1.

ature, as observed by ^1H NMR measurement. The torsion angles between the central benzene ring and naphthyl groups on the same side were almost perpendicular (89.10 and 89.53°). The other naphthyl ring was at 69.21° to the central phenyl ring. No hydrogen bonding between two hydroxy groups was observed, either intra- or intermolecularly.¹⁰ One of the OH groups was directed toward the bottom benzene ring, probably because of the interaction between protic hydrogen and the π -orbital of the central benzene.¹¹

Photophysical Properties of Tris(hydroxynaphthyl)benzenes and Their Related Compounds. 1,3,5-Tri-1-naphthylbenzene (**3**), with an unsubstituted structural form, might have efficient conjugation relative to naphthalene between the three naphthyl groups and the central benzene moiety. However, the absorption maximum of **3** was observed at ca. 296 nm, which was only a small shift from simple naphthalene **8** (278 nm), because the structure could not be planar due to a steric hindrance.³ Photophysical data of various types of trinaphthylbenzenes **1–5** and naphthalene derivatives **6–8** (Chart 1) are shown in Table 1, and electronic absorption spectra are shown in Figure 2. Since the shapes of spectra of examined molecules were similar, we discussed the photophysical properties by using absorption and emission maxima.¹² The OH-substituted compound **1** at the *peri*-positions had an absorption maximum of ca. 320 nm, which was bathochromically shifted compared with that of the unsub-

stituted **3** ($\Delta(\mathbf{3} \rightarrow \mathbf{1}) = 24 \text{ nm}$). The *para*-OH-substituted compound **4**, which is an isomer of the *peri*-compound **1**, showed almost the same absorption maximum (ca. 316 nm) with that of **1**. In simple naphthalene framework, substitution by an OH group lead to a red shift ($\Delta(\mathbf{8} \rightarrow \mathbf{6}) = 21 \text{ nm}$) with a value approximately equal to those of **1** and **4**. These results indicate that the OH group of **1** has no special effect on absorption.

The emission spectra and data for compounds **1–8** are shown in Figure 3 and Table 1. Surprisingly, compound **1** had a characteristic feature for emission, which was observed at around 446 nm, bathochromically shifted by 86 nm from that of unsubstituted compound **3**. As substitution by an OH group in a simple naphthalene system showed less shift ($\Delta(\mathbf{8} \rightarrow \mathbf{6}) = 30 \text{ nm}$), the bathochromic shift in **1** was found to be derived from the extra factor based on its characteristic structure. The *para*-OH-substituted compound **4** showed less shift ($\Delta(\mathbf{3} \rightarrow \mathbf{4}) = 32 \text{ nm}$), suggesting the position of the OH group is critical for the emitting properties of a trinaphthylbenzene system.¹³ The observed effect of the OH group was larger on emission than absorption. The methoxy-substituted compound **2** also had a relatively larger shift than the corresponding **5** and **7**, although the degree of the shift was not huge as compared to the hydroxy-substituted compound **1**. Therefore, the protic hydrogen appears to be critical in effectively extending the conjugation of the biaryl system.¹⁴

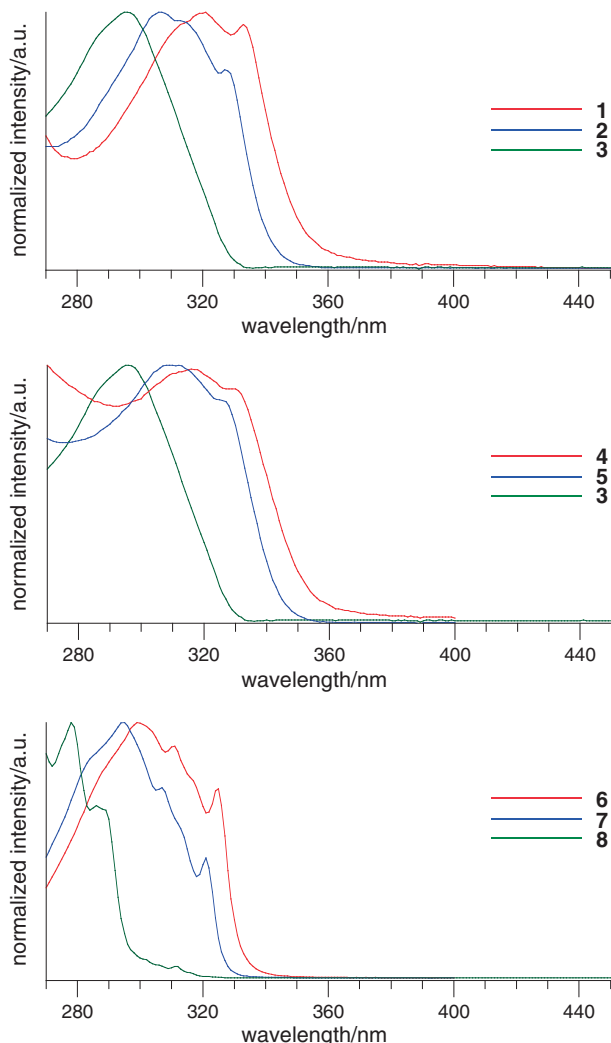


Figure 2. Absorption spectra of 1–8 in DMSO.

Mono(hydroxynaphthyl)benzene. To simplify the discussion of photophysical properties of the trisubstituted benzene **1**, single naphthyl-substituted benzenes **9–13** were examined. The *peri*-OH, or OMe-substituted compounds **9** and **10**, and the *para*-substituted compounds **12** and **13** were prepared by arylation of 1-naphthol¹⁵ or by the Suzuki–Miyaura coupling reaction.^{4,5} Compounds **9–13** were investigated by UV–vis absorption and emission spectroscopy (Table 2 and Figure 4).¹⁶ The *peri*-OH-substituted naphthylbenzene **9** showed emission maximum at a much longer wavelength (422 nm) than the parent unsubstituted compound **11** (352 nm), and significant bathochromic shift of emission from **11** ($\Delta(\mathbf{11} \rightarrow \mathbf{9}) = 70$ nm). However, the *para*-OH-substituted compound **12** showed a normal emission wavelength (386 nm) because the shift ($\Delta(\mathbf{11} \rightarrow \mathbf{12}) = 34$ nm) was almost the same value as that of **6** from **8** ($\Delta(\mathbf{8} \rightarrow \mathbf{6}) = 30$ nm). These results mean that the singly-substituted compound can be used to clarify the mechanism of the “abnormal” photophysical properties of the *peri*-OH-substituted biaryl system.

Theoretical Calculations. Compounds **9–13** were theoretically investigated to understand the origin of the unexpected bathochromic shift of the *peri*-OH- or *peri*-OMe-substituted

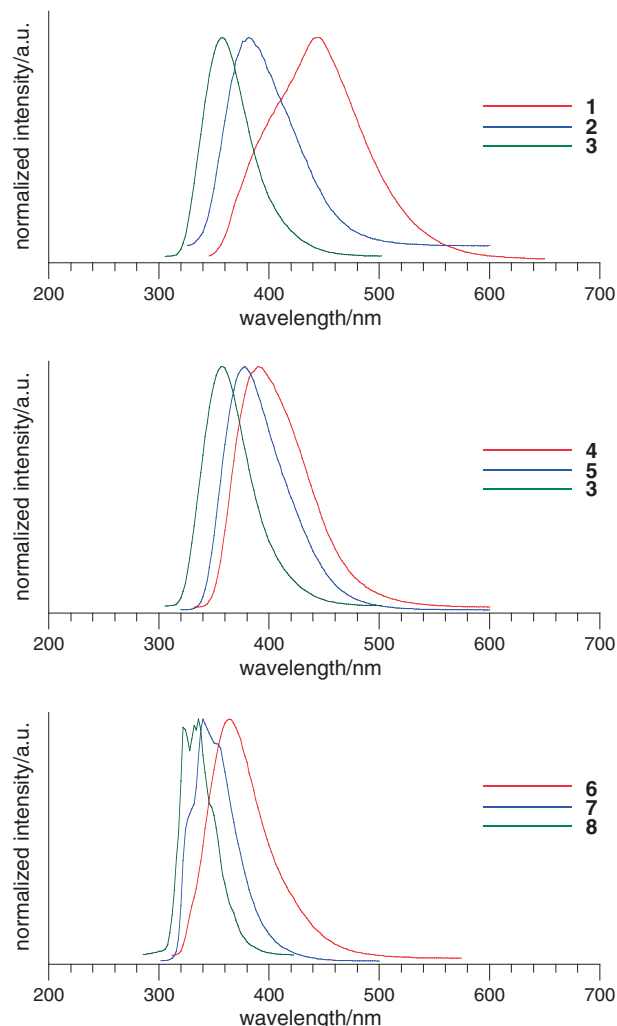
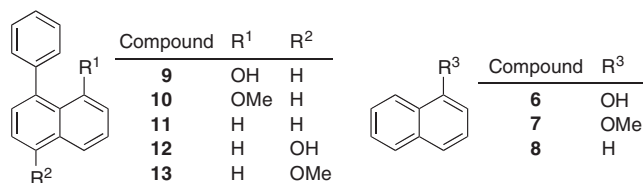


Figure 3. Emission spectra of 1–8 in DMSO excited at 334 nm for **1**, 306 nm for **2**, 298 nm for **3**, 320 nm for **4**, 316 nm for **5**, 300 nm for **6**, 296 nm for **7**, and 278 nm for **8**.

Table 2. Photophysical Data of Mononaphthylbenzene Derivatives

Compound	Absorption		Emission	
	λ_{\max}/nm	$\epsilon/10^4 \text{M}^{-1} \text{cm}^{-1}$	$\lambda_{\max}(\lambda_{\text{ex}})/\text{nm}$	Φ
9	331	1.79	422 (312)	0.01
10	303	0.83	382 (304)	0.05
11	291	1.09	352 (294)	0.23
12	317	1.29	386 (316)	0.09
13	301	1.37	374 (308)	0.16
6	299	0.579	366 (300)	0.07
7	295	0.717	340 (296)	0.38
8	278	0.608	336 (278)	0.31



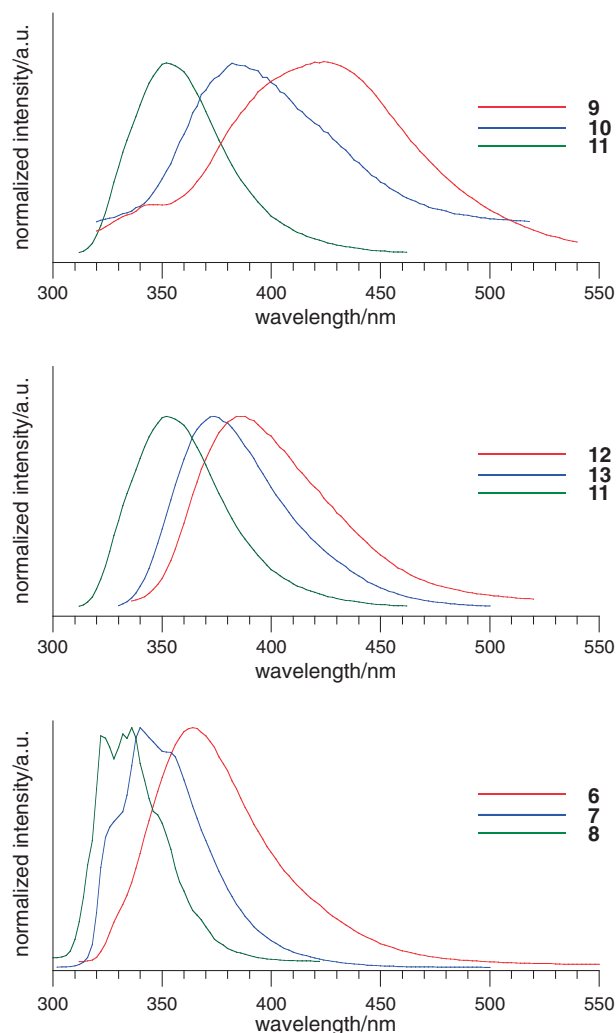


Figure 4. Emission spectra of **6–13** in DMSO excited at 312 nm for **9**, 304 nm for **10**, 294 nm for **11**, 316 nm for **12**, 308 nm for **13**, 300 nm for **6**, 296 nm for **7**, and 278 nm for **8**.

compounds **9** and **10**. The calculated optimized structures of the ground states (S_0) and the excited states (S_1) are shown in Table 3. MO diagrams of the higher singly occupied MOs (SOMOs) in the S_1 states, which correspond to LUMOs in the S_0 state, are included. We will focus on the substituent dependencies of emission wavelengths from the S_1 state. The calculation for *para*-OH-substituted compound **12** gave two stable conformers, **12-R** and **12-L**, in which the O–H bonds point in different directions, as shown in Table 3.¹⁷ The **12-R** form was more stable than the **12-L** form ($E(L) - E(R) = 1.75 \text{ kcal mol}^{-1}$) at the S_0 state, probably because there was less steric hindrance between *ana*-hydrogen and the OH group in **12-R**. The more stable species in the *peri*-OMe-substituted compound **10** was also the R-type ($E(L) - E(R) = 2.20 \text{ kcal mol}^{-1}$), due to a lower steric hindrance between Ome and the phenyl group. On the other hand, in the case of the *peri*-OH-substituted compound **9**, the L-type was more stable than the R-type ($E(L) - E(R) = -2.94 \text{ kcal mol}^{-1}$) despite its larger steric hindrance.¹⁸ The electric interaction of OH with the phenyl group would prefer the structure of **9-L**, and the details are discussed later. Also in the S_1 state, **9-L** was much more

stable than **9-R** ($E(L) - E(R) = -8.28 \text{ kcal mol}^{-1}$). These results suggest that the *peri*-OH group controls the excited state more efficiently than the ground state.²⁰

In all S_0 states, the dihedral angles between the naphthyl and phenyl rings were close to perpendicular ($56.4\text{--}92.4^\circ$), while in the S_1 states, the angles became smaller, and the biaryl framework approached a planar shape ($25.7\text{--}35.9^\circ$).²¹ This is because the double-bond character of the C–C bond between naphthyl and phenyl is strengthened by the HOMO \rightarrow LUMO excitation. In fact, an in-phase orbital interaction can be seen in the C–C bonds at higher SOMOs in S_1 states, but not in HOMOs at S_0 states (Table 3 and Supporting Information). The distances between *peri*-carbon in the naphthyl group and *ortho*-carbon in the phenyl group ($C_{\text{Naph-}peri} - C_{\text{Ph-ortho}}$) in S_1 states were shorter than the corresponding distances in S_0 states.²² The structural change to planar in the S_1 state led to a large Stokes shift. The unsubstituted compound **11** and the *para*-OMe-substituted compound **13** had almost the same structures in S_0 and S_1 states, and the calculated Stokes shifts showed almost the same values (60 and 61 nm, respectively).²³ On the other hand, a larger Stokes shift for *peri*-OMe-substituted compound **10** was theoretically estimated (86 nm)²⁴ than those for **11** and **13**. It was noted that *peri*-OMe-substituted compounds **10-R** and **10-L** in S_1 states showed a more planar structure (dihedral angles between naphthyl and phenyl groups of 25.7 and 25.8° , respectively) than that of *para*-OMe-substituted compound **13** (32.8°). To avoid the steric repulsion between the *peri*-substituent and the phenyl group, the aryl-aryl bond rises from the naphthyl plane. That structural change can decrease the dihedral angle and bring the two aryl planes close to planar. In the case of *peri*-OH-substituted **9**, the R-type compound had a small dihedral angle (27.8°), while **9-L** showed a larger angle (31.9°) because OH was directed to the phenyl ring. Even in this case, the dihedral angle was less than that of either unsubstituted compound **11** (32.5°) or **12** (R; 33.4° , L; 35.9°). The higher SOMOs in the S_1 states were interesting, showing that *peri*-OH- or *peri*-OMe-substituted compounds **9** and **10** had efficient populations on the phenyl rings as compared to those on the phenyl moiety in unsubstituted compound **11** and *para*-substituted species **12** and **13** (Table 3). Compounds **9** and **10** thus had significant conjugation extended through the biaryl system in S_1 states. The lower orbital energies of the higher SOMO in **10** (**10-R**; 1.85 eV , **10-L**; 1.71 eV) in S_1 states were also confirmed, as compared to the *para*-OMe species **13** (2.13 eV). As a result of changes in the positions or directions of OH or OMe substituents, the variations of lower SOMO energies in the S_1 state, which correspond to HOMO energies in the S_0 state, are smaller than those of higher SOMO energies (see Supporting Information). Thus the stabilization of higher SOMOs is ascribed to a bathochromic shift of the emissions. Efficient conjugation is promoted by the planarity of the structure in **10** as compared to **13**. In addition, in OH-substituted compounds **9** and **12**, the higher SOMO energies of *peri*-OH-form **9** were lower than those of *para*-OH-form **12**. Interestingly, conformer **9-L** had much lower orbital energy (1.67 eV) than **9-R** (1.82 eV), despite the large dihedral angle of **9-L**. This effect is not fully explained by planarity, and thus the through-space interaction between naphthyl and phenyl moieties mediated by

Table 3. Calculated Results of the S_0 min and S_1 min Structures and Higher SOMOs of the S_1 State for 9–13

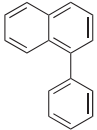


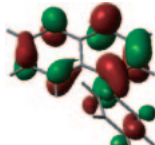
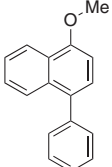
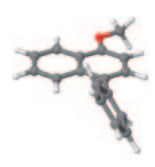
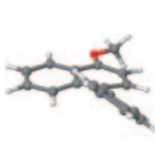
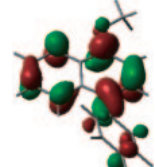
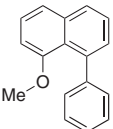
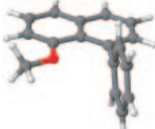
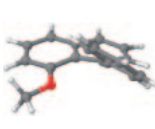
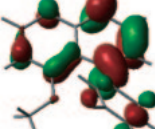
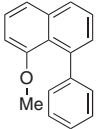
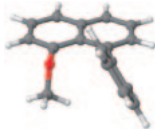
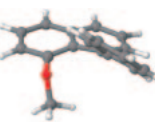
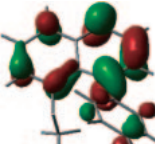
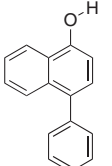
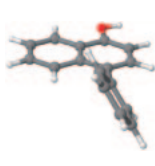
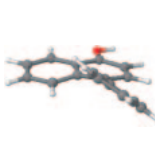
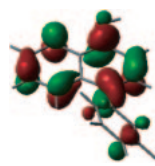
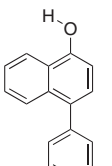
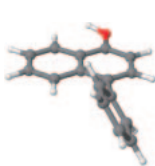
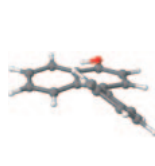
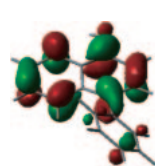
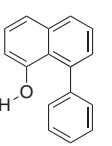
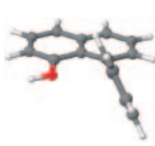
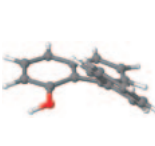
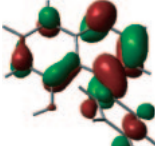
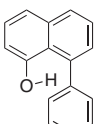
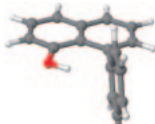
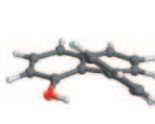
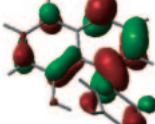
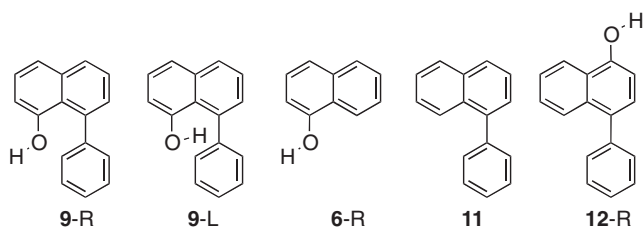
Compound	S_0		S_1		MO diagram of higher SOMO at S_1	Higher SOMO energies of the S_1 state/eV	
	Optimized structure	Dihedral angle of biaryl/ $^\circ$	Optimized structure	Dihedral angle of biaryl/ $^\circ$			
11			57.2		32.5		1.84
13			56.4		32.8		2.13
10-R			92.4		25.7		1.85
	∇	$\Delta E(L - R)$ = 2.20 kcal mol $^{-1}$		$\Delta E(L - R)$ = 2.97 kcal mol $^{-1}$			
10-L			61.9		25.8		1.71
12-R			56.6		33.4		2.07
	∇	$\Delta E(L - R)$ = 1.75 kcal mol $^{-1}$		$\Delta E(L - R)$ = 1.19 kcal mol $^{-1}$			
12-L			57.1		35.9		1.91
9-R			66.7		27.8		1.82
	∧	$\Delta E(L - R)$ = -2.94 kcal mol $^{-1}$		$\Delta E(L - R)$ = -8.28 kcal mol $^{-1}$			
9-L			91.7		31.9		1.67

Table 4. Charges of the H for OH, Phenyl-Ring, and Naphthyl-Ring Calculated from the NAO Atomic Charges^{a)}

Compound	State	R/L	H of OH	Ph	Naph
9	S ₀	R	0.499	0.008	0.238
		L	0.523	-0.005	0.246
	S ₁	R	0.496	0.011	0.230
		L	0.520	-0.060	0.283
6	S ₀	R	0.501	—	0.008
	S ₁	R	0.498	—	-0.003
11	S ₀	—	—	0.001	-0.242
	S ₁	—	—	-0.005	-0.231
12	S ₀	R	0.501	-0.003	0.259
	S ₁	R	0.498	-0.018	0.256

a) The charge of Ph was defined as a sum of atomic charges on atoms of phenyl (C₆H₅) and that of Naph was done as a sum of atomic charges on atoms of C₁₀H₆ in naphthyl moiety.

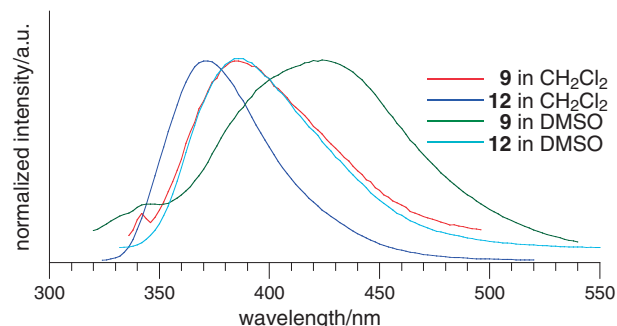


the OH group would be important. In the *peri*-OH compound **9**, the L-type, which has a lower orbital energy, was a dominant conformer, hence, the origin of the stability of **9**-L was next investigated by using the relationship between structure and atomic charge.

The charges of the H of OH, phenyl-ring, and naphthyl-ring calculated from the natural atomic orbital (NAO) charges in the S₀ and S₁ states of naphthol **6**-R, *peri*-substituted **9**-L, and *para*-substituted **12**-R, which are more stable conformers, are shown in Table 4.²⁵ The unsubstituted phenylnaphthalene and the conformation isomer of the main compound **9**-L (**11** and **9**-R) are also included in Table 4. In **9**-L, the positive charge was localized at the naphthyl ring and the hydroxy proton, and the negative charge was localized at the phenyl ring. The charge-separated state in **9**-L was more highly polarized in the S₁ state than in the S₀ state, so the focus was on the charges in the S₁ states to compare the compounds.

Next, the NAO charges of **6**-R, **9**-L, and **11** in the S₁ states were compared to investigate how the phenyl group and hydroxy group affect the charge-separated state. One of the large differences among them was the charge at the naphthyl ring {**6**-R; neutral (S₁; -0.003), **9**-L; positive (S₁; 0.283), and **11**; negative (S₁; -0.231)}. In **6**-R, the positive charge of the hydroxy proton was smaller than that in **9**-L. In **11**, the charge of the phenyl ring was almost neutral, while **9**-L had a negative charge at the phenyl ring. The presence of both the phenyl group and the hydroxy group played an important role in creating a more highly polarized charge-separated state in **9**-L.

We examined the importance of the substituting position of the hydroxy group by comparing the compounds *peri*-form **9**-L and *para*-form **12**-R. In the S₁ state, although the charges at the naphthyl ring were equally positive in both **9**-L and **12**-R, the negative charge at the phenyl ring in **9**-L was about three times

**Figure 5.** Solvent effect on emission spectra of **9** and **12** excited at 306 nm for **9** (CH₂Cl₂), 304 nm for **12** (CH₂Cl₂), 312 nm for **9** (DMSO), and 316 nm for **12** (DMSO).

higher than that in **12**-R. These results show that the hydroxy group in the *peri*-position is an important factor in inducement of the negative charge at the phenyl ring.

To determine how the hydroxy group interacts with the phenyl group, we compared the NAO charges of **9**-L and **9**-R, with hydroxy protons that orient toward and away from the phenyl ring, respectively. The charge of the phenyl ring in **9**-L was negative while that in **9**-R was positive. This means that the hydroxy group electrostatically interacts with the phenyl group through the hydroxy proton directed to the phenyl ring. In fact, the positive charge of the hydroxy proton in **9**-L was larger than that in **9**-R. This electrostatic interaction contributes to lowering the higher SOMO energy (1.67 eV) in **9**-L, despite the steric hindrance between the hydroxy proton and the phenyl group.

The calculation data in Tables 3 and 4 reveal that the relationship between the phenyl group and the hydroxy group in the *peri*-position in the naphthyl ring generates electrostatic interaction, which is mediated by the hydroxy proton. This interaction leads to a highly polarized charge-separated state and increases planarity between phenyl and naphthyl rings, and could contribute to a large bathochromic shift for emission. Those factors could extend the conjugation of the biaryl system, especially in S₁ states.

Effect of Solvents and Substituents on Mono(hydroxy-naphthyl)benzene. The solvent effect on the emission of **9** and **12** is shown in Figure 5. Compound **9** gave an emission maximum at 386 nm in dichloromethane, and 422 nm in DMSO ($\lambda_{\text{em}}(\text{DMSO}) - \lambda_{\text{em}}(\text{CH}_2\text{Cl}_2) = 36$ nm). DMSO showed a bathochromic shift and effectively stabilized the polarized S₁ state. In the case of **12**, less bathochromic shift was found in DMSO (λ_{em} ; 386 nm in DMSO, 368 nm in CH₂Cl₂, $\lambda_{\text{em}}(\text{DMSO}) - \lambda_{\text{em}}(\text{CH}_2\text{Cl}_2) = 18$ nm), because less polarization was generated in **12** in the S₁ state. These results are consistent with the calculation results and suggest that the charged transient is a key factor for emission in this system. A similar solvent effect was observed in trisubstituted benzene **1**.²⁶ Compound **1** gave an emission maximum at 378 nm in dichloromethane, and 446 nm in DMSO. Polar solvent (DMSO) showed a bathochromic shift ($\lambda_{\text{em}}(\text{DMSO}) - \lambda_{\text{em}}(\text{CH}_2\text{Cl}_2) = 68$ nm). The *para*-OH-substituted **4** showed less bathochromic shift in DMSO (λ_{em} ; 392 nm in DMSO, 374 nm in CH₂Cl₂, $\lambda_{\text{em}}(\text{DMSO}) - \lambda_{\text{em}}(\text{CH}_2\text{Cl}_2) = 18$ nm).

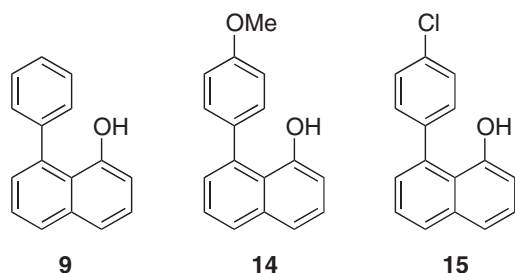


Chart 2.

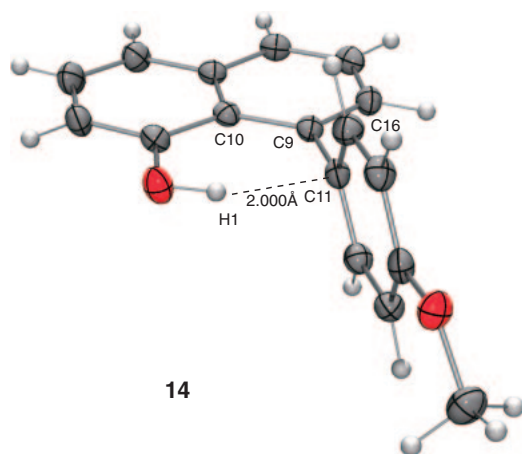


Figure 6. ORTEP drawing of **14**. Selected torsion angle and distance: C(10)–C(9)–C(11)–C(16) 84.36°, H(1)–C(11) 2.000 Å.

This suggests that the highly polarized charge-separated state is generated in **1** as well as in **9**.

The substituent effect of *peri*-OH-naphthylbenzene was investigated. We prepared methoxy- and chloro-substituted compounds **14** and **15**, respectively, as shown in Chart 2. While compound **9** was a liquid, the substituted derivatives **14** and **15** were solidified to give a crystal suitable for X-ray analyses. Their ORTEP drawings are shown in Figures 6 and 7. The torsion angles between the phenyl ring and the naphthyl plane were 84.36° for **14**, and 76.72 and 76.28° for **15**.²⁷ The OH groups on the naphthyl moiety were directed toward the phenyl ring, as predicted by theoretical calculation (Table 3). This can presumably be ascribed to an electronic interaction between the phenyl and the OH groups. The distances between the H and the *ipso*-carbon were 2.000 Å for **14** and 2.192 Å for **15**.

The OMe- and Cl-substituents on the phenyl ring of **9** affected the emission spectra in an interesting manner (Figure 8). The methoxy-substituted compound **14** showed emission (398 nm) at a shorter wavelength than the unsubstituted compound **9** (422 nm), although the methoxy group generally causes an emission at a longer wavelength. This result also supports the polarization mechanism in the *peri*-substituted 1-arylnaphthalene system. The methoxy group suppresses polarization with its electron-donating effect. The chloro-substituted compound **15** showed its emission maxima at a slightly longer wavelength (426 nm) than **9**, probably because of its electron-withdrawing characteristics.

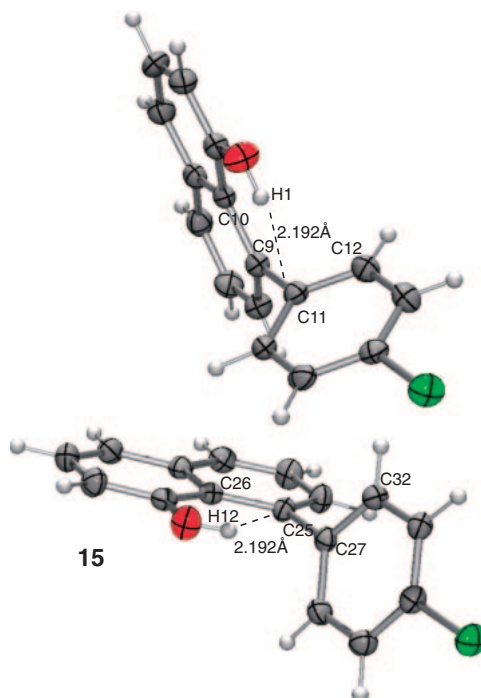


Figure 7. ORTEP drawings of **15**. Selected torsion angles and distances: C(10)–C(9)–C(11)–C(12) 76.72°, C(26)–C(25)–C(27)–C(32) 76.28°, H(1)–C(11) 2.192 Å, H(12)–C(27) 2.192 Å.

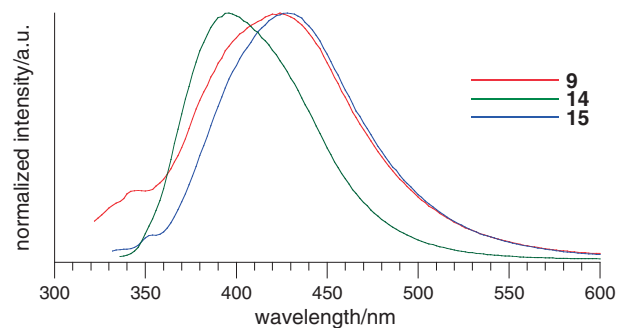


Figure 8. Emission spectra of **9**, **14**, and **15** in DMSO excited at 312 nm for **9**, 320 nm for **14**, and 320 nm for **15**.

Conclusion

A *peri*-OH-substituted 1-arylnaphthalene system showed characteristic photophysical properties, particularly on emission. The conjugation of biaryl systems was effectively enhanced by the hydroxy group at the *peri*-position in the excited state. The hydrogen on the *peri*-OH group interacted with the phenyl ring on naphthalene and induced polarity in the molecule, while the methoxy substituent was not directed to the phenyl ring due to its steric hindrance. Compared with the lower SOMO energy, the higher SOMO energy was relatively lowered by a polarized transient structure, and thus a bathochromic shift was observed. The *peri*-position of the OH-substituent was critical for the emission wavelength, while the *para*-substituted compound did not show this property. 1,3,5-Tris(*peri*-hydroxynaphthyl)benzene (**1**) gave an interesting blue emission and significant bathochromic shifts were

observed in the emission spectra. In the compounds **1** and **9**, the substituted position of OH was quite critical because the hydroxy group mediated the different π -systems by through-space interaction to stabilize the excited state.

Experimental

General. IR spectra were recorded as thin films or as solids in KBr pellets. ^1H and ^{13}C NMR spectra were obtained with a 400 and 100 MHz spectrometer, respectively, with TMS as an internal standard. UV-vis spectra and emission spectra were obtained at room temperature using 0.01 mM in DMSO unless otherwise specified. Absorption spectra of naphthalene derivatives **6–8** were obtained using 0.2 mM in DMSO.

Materials. 1-Hydroxynaphthalene (**6**), 1-methoxynaphthalene (**7**), naphthalene (**8**), 1-phenylnaphthalene (**11**), 1,3,5-tribromobenzene, bromobenzene, $[\text{Pd}(\text{PPh}_3)_4]$, $\text{B}(\text{OMe})_3$, and BBr_3 were commercially available. 8-Methoxy-1-naphthylboronic acid **A**,⁶ 1-bromo-4-methoxynaphthalene,²⁸ and 5-methoxy-1-naphthol²⁹ were prepared by known methods. 1,3,5-Tri-1-naphthylbenzene (**3**),³⁰ 8-phenyl-1-naphthol (**9**),¹⁵ and 4-phenyl-1-naphthol (**12**)³¹ were prepared by Suzuki–Miyaura coupling reaction⁵ and their spectra were exactly matched to the reported data. Other compounds were prepared as shown below.

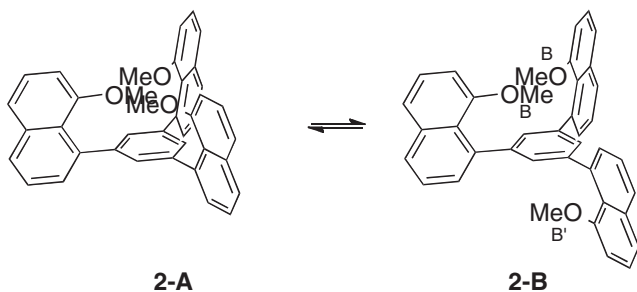
1,3,5-Tris(8-methoxy-1-naphthyl)benzene (2): To a suspension of 8-methoxy-1-naphthylboronic acid (16.5 mmol) in toluene (15 mL), EtOH (25 mL), water (15 mL), and Na_2CO_3 (25 mmol) were added and the mixture was stirred for 1 h at room temperature. Then, the mixture was added to a solution of 1,3,5-tribromobenzene (5.0 mmol) and $[\text{Pd}(\text{PPh}_3)_4]$ (0.5 mmol) in toluene (10 mL) and stirred for 24 h at 90 °C.⁵ The mixture was cooled to 0 °C and water (30 mL) was added. The mixture was extracted with ethyl acetate (3 \times 30 mL). The combined organic layer was dried over MgSO_4 and evaporated. The residue was purified by column chromatography (hexane/EtOAc, 50:50) and recrystallization (hexane) to give the product as a white solid (2.34 g, 86%). mp: 155–158 °C; IR: (neat) 1577, 1269 cm^{-1} .

^1H NMR (600 MHz, CDCl_3 , 60 °C) (**2-A–2-B** fast equilibrium, Scheme 3): δ 7.75 (m, 3H), 7.50–7.40 (m, 6H), 7.45 (t, $J = 8.4$ Hz, 3H), 7.35 (t, $J = 7.8$ Hz, 3H), 7.30 (s, 3H), 6.79 (d, $J = 7.8$ Hz, 3H), 3.65 (s, 9H); ^{13}C NMR (150 MHz, CDCl_3 , 60 °C): δ 157.3, 142.2, 140.1, 136.2, 129.7, 127.5, 127.3, 125.8, 125.5, 124.1, 121.4, 106.5, 55.2. ^1H NMR (400 MHz, CDCl_3 , 20 °C) (mixture of **2-A** and **2-B**): δ 7.78 (d, $J = 9.0$ Hz), 7.60–7.28 (m), 6.87–6.70 (m), 3.70 (s), 3.67 (s), 3.58 (s); ^{13}C NMR (100 MHz, CDCl_3 , 20 °C): δ 157.0, 156.8, 142.1,

141.8, 141.5, 139.8, 135.9, 129.7, 128.9, 127.7, 127.4, 127.2, 126.6, 125.8, 125.6, 125.4, 125.2, 123.7, 123.5, 121.1, 106.0, 105.9, 105.8, 55.3, 55.0, 54.4. ^1H NMR (600 MHz, CDCl_3 , –60 °C) (**2-A:2-B** = ca. 1:1): δ 7.84 (m), 7.58–7.34 (m), 6.85 (d, $J = 7.8$ Hz), 6.83 (d, $J = 7.8$ Hz), 3.76 (s), 3.71 (s), 3.67 (s); ^{13}C NMR (150 MHz, CDCl_3 , –60 °C): δ 156.5, 156.2, 156.1, 141.6, 141.4, 141.2, 139.2, 135.42, 135.38, 135.32, 129.6, 129.4, 129.2, 127.6, 127.25, 127.21, 127.17, 127.11, 126.7, 125.80, 125.77, 125.74, 125.6, 125.4, 125.3, 122.78, 122.75, 122.67, 120.8, 120.7, 105.2, 105.0, 55.1, 54.7, 54.2; MS (EI, 70 eV): m/z 546 (M^+ , 100); HRMS (EI, 70 eV): calcd for $\text{C}_{39}\text{H}_{30}\text{O}_3$ 546.2195, found m/z 546.2189 (M^+). Anal. Calcd for $\text{C}_{39}\text{H}_{30}\text{O}_3$: C, 85.69; H, 5.53%. Found: C, 85.43; H, 5.59%.

1,3,5-Tris(8-hydroxy-1-naphthyl)benzene (1): To a solution of 1,3,5-tris(8-methoxy-1-naphthyl)benzene (2.0 mmol) in CH_2Cl_2 (12 mL) was slowly added BBr_3 (1.0 M in CH_2Cl_2 , 6.6 mL) at –78 °C. The mixture was stirred at –78 °C to rt for 8 h. The mixture was cooled to 0 °C and quenched by water. The mixture was extracted with ethyl acetate (3 \times 10 mL). The combined organic layer was dried over MgSO_4 and evaporated. The residue was purified by flash column chromatography (hexane/EtOAc, 70:30) to give the product as a white solid (0.87 g, 87%). Further, recrystallization from CH_2Cl_2 /hexane afforded crystals suitable for X-ray structure analysis. Crystallographic data have been deposited with Cambridge Crystallographic Data Centre: Deposition number CCDC-803341 for compound **1**. Copies of the data can be obtained free of charge via <http://www.ccdc.cam.ac.uk/conts/retrieving.html> (or from the Cambridge Crystallographic Data Centre, 12, Union Road, Cambridge, CB2 1EZ, U.K.; Fax: +44 1223 336033; e-mail: deposit@ccdc.cam.ac.uk). Mp: 256–264 °C; IR (KBr): 3510, 3432 (OH) cm^{-1} ; ^1H NMR (600 MHz, $\text{DMSO}-d_6$, 70 °C): δ 8.97 (brs, 3H), 7.81 (d, 3H, $J = 7.8$ Hz), 7.48 (t, 3H, $J = 7.8$ Hz), 7.41 (d, 3H, $J = 7.8$ Hz), 7.39 (d, 3H, $J = 7.8$ Hz), 7.32 (s, 3H), 7.31 (t, 3H, $J = 7.8$ Hz), 6.87 (d, 3H, $J = 7.8$ Hz); ^{13}C NMR (150 MHz, $\text{DMSO}-d_6$, 70 °C): δ 153.9, 140.7, 138.3, 135.6, 128.3, 127.7, 127.2, 126.0, 124.6, 121.6, 119.1, 110.1. ^1H NMR (600 MHz, $\text{DMSO}-d_6$, 22 °C): δ 9.66 (brs, 1H), 9.36 (brs, 2H), 7.81 (m, 3H), 7.48 (m, 3H), 7.44–7.35 (m, 6H), 7.31 (t, 3H, $J = 7.8$ Hz), 7.29 (s, 3H), 6.85 (brs, 3H); ^{13}C NMR (150 MHz, $\text{DMSO}-d_6$, 22 °C): δ 154.3, 140.6, 139.0, 135.9, 128.9, 128.6, 127.5, 126.4, 125.1, 121.7, 119.3, 110.1. This compound has conformation shown in Chart 3 at room temperature.

MS (EI, 70 eV): m/z 504 (M^+ , 100.0); HRMS (EI, 70 eV): calcd for $\text{C}_{36}\text{H}_{24}\text{O}_3$ 504.1725, found m/z 504.1723 (M^+). Anal. Calcd for $\text{C}_{36}\text{H}_{24}\text{O}_3$: C, 85.69; H, 4.79%. Found: C, 85.50; H, 4.84%.



Scheme 3.

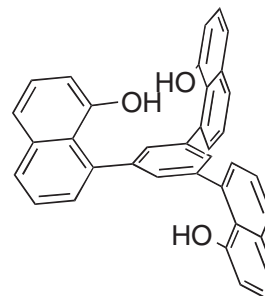


Chart 3.

4-Methoxy-1-naphthylboroxin (B): To a solution of 1-bromo-4-methoxynaphthalene²⁸ (40 mmol) in toluene (60 mL) and THF (15 mL) at -78°C was slowly added *n*-BuLi (1.6 M in hexane, 30 mL, 48 mmol) for the period of 1.5 h. After the reaction mixture was stirred for another 1 h at -78°C , B(Oi-Pr)₃ (48 mmol) was slowly added for the period of 30 min at the same temperature. The mixture was allowed to warm to 0°C . HCl(aq) solution (2 M, 50 mL) and EtOAc (50 mL) was added to the mixture and it was stirred (for ca. 1 h) until the organic layer became clear. The mixture was extracted with EtOAc (3 \times 30 mL). The combined organic layer was washed with sat. NaHCO₃(aq) and brine, dried over MgSO₄ and evaporated. The residue was washed with hexane and filtrated to give a white solid (6.4 g, 87%). Mp: 250–252 $^{\circ}\text{C}$; IR (KBr): 1574 (aryl), 1512 (aryl), 1238 (C–O–C) cm^{-1} ; ¹H NMR (400 MHz, CDCl₃): δ 9.30 (d, 1H, *J* = 8.4 Hz), 8.64 (d, 1H, *J* = 7.9 Hz), 8.40 (dd, 1H, *J* = 8.5, 1.0 Hz), 7.68 (ddd, 1H, *J* = 8.5, 6.8, 1.6 Hz), 7.56 (ddd, 1H, *J* = 8.4, 6.8, 1.0 Hz), 7.02 (d, 1H, *J* = 7.9 Hz), 4.12 (s, 3H); ¹³C NMR (100 MHz, CDCl₃): δ 159.3, 139.0, 138.6, 128.0, 127.2, 125.7, 125.0, 122.3, 103.4, 55.6. MS (EI, 70 eV): *m/z* 552 (M⁺, 100), 158 (86), 143 (30), 115 (65); HRMS (EI, 70 eV): calcd for C₃₃H₂₇B₃O₆ 552.2087, found *m/z* 552.2091 (M⁺). Anal. Calcd for C₃₃H₂₇B₃O₆: C, 71.80; H, 4.93%. Found: C, 71.52; H, 4.93%.

1,3,5-Tris(4-methoxy-1-naphthyl)benzene (5): To a suspension of 4-methoxy-1-naphthylboroxin (5.2 mmol) in toluene (10 mL), EtOH (20 mL), water (12 mL), and Na₂CO₃ (20 mmol) were added and the mixture was stirred for 1 h at room temperature. Then, the mixture was added to a solution of 1,3,5-tribromobenzene (4.0 mmol) and [Pd(PPh₃)₄] (0.4 mmol) in toluene (10 mL) and stirred for 17 h at 90°C .⁵ The mixture was cooled to 0°C and water (30 mL) was added. The mixture was extracted with ethyl acetate (3 \times 30 mL). The combined organic layer was dried over MgSO₄ and evaporated. The residue was purified by flash column chromatography (hexane/EtOAc, 95:5) to give the product as a white solid (1.56 g, 71%). Mp: 218–221 $^{\circ}\text{C}$; IR (KBr): 1585 (aryl) cm^{-1} ; ¹H NMR (400 MHz, CDCl₃): δ 8.35 (m, 3H), 8.18 (m, 3H), 7.67 (s, 3H), 7.50 (m, 9H), 6.90 (d, 3H, *J* = 8.0 Hz), 4.04 (s, 9H); ¹³C NMR (100 MHz, CDCl₃): δ 155.0, 140.7, 132.43, 132.4, 130.6, 127.2, 126.6, 125.8, 125.7, 125.1, 122.2, 103.5, 55.6; MS (EI, 70 eV): *m/z* 546 (M⁺, 100); HRMS (EI, 70 eV): calcd for C₃₉H₃₀O₃ 546.2195, found *m/z* 546.2191 (M⁺). Anal. Calcd for C₃₉H₃₀O₃: C, 85.69; H, 5.53%. Found: C, 85.44; H, 5.50%.

1,3,5-Tris(4-hydroxy-1-naphthyl)benzene (4): To a solution of 1,3,5-tris(4-methoxy-1-naphthyl)benzene (0.56 mmol) in CH₂Cl₂ (3 mL), was slowly added BBr₃ (1.0 M in CH₂Cl₂, 1.8 mL) at -78°C . The mixture was stirred at -78°C to rt for 8 h. The mixture was cooled to 0°C and quenched by water. The mixture was extracted with ethyl acetate (3 \times 10 mL). The combined organic layer was dried over MgSO₄ and evaporated. The residue was purified by flash column chromatography (hexane/EtOAc, 60:40) to give the product as a white solid (0.254 g, 90%). Mp: decomposition 295 $^{\circ}\text{C}$; IR (KBr): 3533 (OH), 1585 cm^{-1} ; ¹H NMR (400 MHz, DMSO-*d*₆): δ 10.35 (brs, 3H), 8.23 (dd, *J* = 8.3, 1.1 Hz, 3H), 8.08 (d, *J* = 8.5 Hz, 3H), 7.55 (ddd, *J* = 8.5, 6.8, 1.1 Hz, 3H), 7.51 (s, 3H), 7.49 (m, 3H), 7.47 (d, *J* = 7.8 Hz, 3H), 6.97 (d, *J* = 7.8 Hz, 3H); ¹³C NMR (100 MHz, DMSO-*d*₆): δ 153.1, 140.6, 131.9, 129.9,

129.9, 127.9, 126.8, 125.0, 124.8, 124.7, 122.6, 107.9; MS (EI, 70 eV): *m/z* 504 (M⁺, 100.0); HRMS (EI, 70 eV): calcd for C₃₆H₂₄O₃ 504.1725, found *m/z* 504.1732 (M⁺).

1-Methoxy-8-phenylnaphthalene (10): To a suspension of 8-methoxy-1-naphthylboronic acid (5.5 mmol) in toluene (15 mL), EtOH (25 mL), water (15 mL), and Na₂CO₃ (7.5 mmol) were added and the mixture was stirred for 1 h at room temperature. Then, the mixture was added to a solution of bromobenzene (5 mmol) and [Pd(PPh₃)₄] (0.25 mmol) in toluene (10 mL) and stirred for 3 h at 90°C .⁵ The mixture was cooled to 0°C and water (30 mL) was added. The mixture was extracted with ethyl acetate (3 \times 10 mL). The combined organic layer was dried over MgSO₄ and evaporated. The residue was purified by column chromatography (hexane). Further purification was performed by distillation under reduced pressure to give the product as a colorless liquid (0.90 g, 78%). Bp: 150 $^{\circ}\text{C}/0.2$ mmHg; IR (neat): 1577 (aryl), 1253 (C–O–C) cm^{-1} ; ¹H NMR (400 MHz, CDCl₃): δ 7.81 (d, *J* = 8.0 Hz, 1H), 7.50 (d, *J* = 8.0 Hz, 1H), 7.46 (t, *J* = 8.0 Hz, 1H), 7.40 (t, *J* = 8.0 Hz, 1H), 7.37–7.28 (m, 5H), 7.27 (d, *J* = 8.0 Hz, 1H), 6.78 (d, *J* = 8.0 Hz, 1H), 3.48 (s, 3H); ¹³C NMR (100 MHz, CDCl₃): δ 156.7, 145.4, 139.0, 135.7, 129.0, 128.7, 127.6, 126.6, 126.0, 125.7, 125.4, 123.5, 121.2, 106.2, 55.2; MS (EI, 70 eV): *m/z* 234 (M⁺, 100), 218 (52); HRMS (EI, 70 eV): calcd for C₁₇H₁₄O 234.1045, found *m/z* 234.1041 (M⁺). Anal. Calcd for C₁₇H₁₄O: C, 87.15; H, 6.02%. Found: C, 87.10; H, 6.01%.

1-Methoxy-4-phenylnaphthalene (13): To a suspension of 4-methoxy-1-naphthylboroxin (1.2 mmol) in toluene (5 mL), EtOH (15 mL), water (9 mL), and Na₂CO₃ (5.0 mmol) were added and the mixture was stirred for 1 h at room temperature. Then, the mixture was added to a solution of bromobenzene (3.0 mmol) and [Pd(PPh₃)₄] (0.15 mmol) in toluene (10 mL) and stirred for 5 h at 90°C .⁵ The mixture was cooled to 0°C and water (30 mL) was added. The mixture was extracted with ethyl acetate (3 \times 30 mL). The combined organic layer was dried over MgSO₄ and evaporated. The residue was purified by flash column chromatography (hexane/EtOAc, 95:5) to give the product as a colorless liquid (0.51 g, 71%). Bp: 170 $^{\circ}\text{C}/0.6$ mmHg; IR (neat): 1238 (C–O–C) cm^{-1} ; ¹H NMR (600 MHz, CDCl₃): δ 8.34 (m, 1H), 7.86 (m, 1H), 7.49 (ddd, *J* = 7.8, 6.6, 1.2 Hz, 1H), 7.48–7.46 (m, 4H), 7.44 (ddd, *J* = 7.8, 6.6, 1.2 Hz, 1H), 7.40 (m, 1H), 7.33 (d, *J* = 7.8 Hz, 1H), 6.87 (d, *J* = 7.8 Hz, 1H), 4.04 (s, 3H); ¹³C NMR (100 MHz, CDCl₃): δ 155.0, 140.9, 132.7, 132.5, 130.3, 128.2, 126.9, 126.8, 126.5, 125.8, 125.7, 125.1, 122.2, 103.4, 55.6; MS (EI, 70 eV): *m/z* 234 (M⁺, 100), 219 (M⁺ – CH₃, 38), 191 (38); HRMS (EI, 70 eV): calcd for C₁₇H₁₄O 234.1045, found *m/z* 234.1043 (M⁺). Anal. Calcd for C₁₇H₁₄O: C, 87.15; H, 6.02%. Found: C, 86.96; H, 6.01%.

8-(4-Methoxyphenyl)-1-naphthol (14): To a suspension of CsCO₃ (10 mmol), which was predried under reduced pressure for 2 h at room temperature, in DMF (25 mL) were added PdCl₂ (0.13 mmol), 1-naphthol (5.0 mmol), and *p*-iodoanisole (6.0 mmol).⁵ The mixture was stirred for 21 h at 110°C . The mixture was cooled to 0°C , and then water was added. The mixture was extracted with ethyl acetate (3 \times 20 mL). The combined organic layer was washed with water (3 \times 20 mL) and dried over MgSO₄. After filtration, the solvent was

evaporated and purified by column chromatography (hexane/EtOAc, 80:20). Further purification was performed by distillation under reduced pressure to give the product as a pale yellow solid (0.29 g, 23%). Further, recrystallization from CH₂Cl₂/hexane afforded crystals suitable for X-ray structure analysis. Crystallographic data have been deposited with Cambridge Crystallographic Data Centre: Deposition number CCDC-803339 for compound **14**. Copies of the data can be obtained free of charge via <http://www.ccdc.cam.ac.uk/conts/retrieving.html> (or from the Cambridge Crystallographic Data Centre, 12, Union Road, Cambridge, CB2 1EZ, U.K.; Fax: +44 1223 336033; e-mail: deposit@ccdc.cam.ac.uk). Mp: 100–101 °C; IR (KBr): 3464 (OH), 1516 cm⁻¹; ¹H NMR (400 MHz, CDCl₃): δ 7.83 (d, *J* = 8.0 Hz, 1H), 7.49 (d, *J* = 8.0 Hz, 1H), 7.44 (d, *J* = 8.8 Hz, 2H), 7.42 (t, *J* = 8.0 Hz, 1H), 7.39 (t, *J* = 8.0 Hz, 1H), 7.18 (d, *J* = 8.0 Hz, 1H), 7.04 (d, *J* = 8.8 Hz, 2H), 6.90 (d, *J* = 8.8 Hz, 1H), 5.66 (s, 1H), 3.89 (s, 3H); ¹³C NMR (100 MHz, CDCl₃): δ 159.8, 153.2, 135.7, 135.7, 132.9, 130.7, 128.7, 128.5, 126.8, 124.8, 121.5, 120.9, 114.4, 111.6, 55.4; MS (EI, 70 eV): *m/z* 250 (M⁺, 100); HRMS (EI, 70 eV): calcd for C₁₇H₁₄O₂ 250.0994, found *m/z* 250.0996 (M⁺). Anal. Calcd for C₁₇H₁₄O₂: C, 81.58; H, 5.64%. Found: C, 81.35; H, 5.66%.

8-(4-Chlorophenyl)-1-naphthol (15): To a suspension of CsCO₃ (10 mmol), which was predried under reduced pressure for 2 h at room temperature, in DMF (25 mL) were added PdCl₂ (0.13 mmol), 1-naphthol (5 mmol), and 1-chloro-4-iodobenzene (6 mmol).⁵ The mixture was stirred for 21 h at 110 °C. The mixture was cooled to 0 °C, and then water was added. The mixture was extracted with ethyl acetate (3 × 20 mL). The combined organic layer was washed with water (3 × 20 mL) and dried over MgSO₄. After filtration, the solvent was evaporated and purified by column chromatography (hexane/EtOAc, 80:20). Further purification was performed by distillation under reduced pressure to give the product as a pale yellow solid (0.37 g, 29%). Further, recrystallization from CH₂Cl₂/hexane afforded crystals suitable for X-ray structure analysis. Crystallographic data have been deposited with Cambridge Crystallographic Data Centre: Deposition number CCDC-803340 for compound **15**. Copies of the data can be obtained free of charge via <http://www.ccdc.cam.ac.uk/conts/retrieving.html> (or from the Cambridge Crystallographic Data Centre, 12, Union Road, Cambridge, CB2 1EZ, U.K.; Fax: +44 1223 336033; e-mail: deposit@ccdc.cam.ac.uk). Mp: 55–57 °C; IR (KBr): 3367 (OH) cm⁻¹; ¹H NMR (400 MHz, CDCl₃): δ 7.86 (d, *J* = 8.0 Hz, 1H), 7.51 (d, *J* = 8.0 Hz, 1H), 7.48–7.41 (m, 5H), 7.40 (t, *J* = 8.0 Hz, 1H), 7.17 (d, *J* = 8.0 Hz, 1H), 6.90 (d, *J* = 8.0 Hz, 1H), 5.20 (s, 1H); ¹³C NMR (100 MHz, CDCl₃): δ 152.6, 140.0, 135.7, 135.0, 134.5, 130.8, 128.9, 128.9, 128.7, 124.9, 121.2, 121.2, 111.9; MS (EI, 70 eV): *m/z* 256 (M⁺ + 2, 34), 254 (M⁺, 100), 218 (M⁺ - Cl, 51), 189 (25); HRMS (EI, 70 eV): calcd for C₁₆H₁₁ClO 254.0498, found *m/z* 254.0504 (M⁺). Anal. Calcd for C₁₆H₁₁ClO: C, 75.45; H, 4.35%. Found: C, 75.31; H, 4.38%.

This work was supported by a Grant-in-Aid for Scientific Research on Innovative Areas (No. 23105525, “Molecular Activation Directed toward Straightforward Synthesis” and

No. 22106527, “Organic Synthesis Based on Reaction Integration. Development of New Methods and Creation of New Substances”), and for Scientific Research (No. 21350074) from the Ministry of Education, Culture, Sports, Science and Technology, Japan. This work was financially supported by the General Sekiyu Research & Development Encouragement & Assistance Foundation. We thank Prof. Y. Wada (Tokyo Inst. Tech.) for the generous discussion and Dr. Nobuko Kanehisa for the valuable advice regarding X-ray crystallography. Thanks are due to Mr. H. Moriguchi, Faculty of Engineering, Osaka University, for assistance in obtaining the MS spectra. H. N. is grateful to the Yoshida Scholarship Foundation and the Global COE Program of Osaka University.

Supporting Information

Experimental procedures, detail assignment of NMR spectra, electronic spectra, listing of absolute energies and geometries for calculated species (PDF). This material is available free of charge on the web at <http://www.csj.jp/journals/bcsj/>.

References

- a) J. M. Tour, *Chem. Rev.* **1996**, *96*, 537. b) M. Kertesz, C. H. Choi, S. Yang, *Chem. Rev.* **2005**, *105*, 3448. c) J. Roncali, *Chem. Rev.* **1997**, *97*, 173. d) I. Kaur, N. N. Stein, R. P. Kopreski, G. P. Miller, *J. Am. Chem. Soc.* **2009**, *131*, 3424. e) J. M. W. Chan, J. R. Tischler, S. E. Kooi, V. Bulović, T. M. Swager, *J. Am. Chem. Soc.* **2009**, *131*, 5659. f) A. Mukherjee, K. Pati, R.-S. Liu, *J. Org. Chem.* **2009**, *74*, 6311. g) K. Itami, Y. Ohashi, J. Yoshida, *J. Org. Chem.* **2005**, *70*, 2778, and references cited in. h) W.-J. Liu, Y. Zhou, Q.-F. Zhou, Y. Ma, J. Pei, *Org. Lett.* **2008**, *10*, 2123.
- a) R. N. Brookins, K. S. Schanze, J. R. Reynolds, *Macromolecules* **2007**, *40*, 3524. b) T. Burnell, J. A. Cella, P. Donahue, A. Duggal, T. Early, C. M. Heller, J. Liu, J. Shiang, D. Simon, K. Slowinska, M. Sze, E. Williams, *Macromolecules* **2005**, *38*, 10667.
- a) J. Trotter, *Acta Crystallogr.* **1961**, *14*, 1135. b) G.-P. Charbonneau, Y. Delugeard, *Acta Crystallogr., Sect. B* **1976**, *32*, 1420. c) A. Karpfen, C. H. Choi, M. Kertesz, *J. Phys. Chem. A* **1997**, *101*, 7426. d) A. C. Benniston, A. Harriman, P. Li, P. V. Patel, C. A. Sams, *J. Org. Chem.* **2006**, *71*, 3481.
- N. Miyaura, A. Suzuki, *Chem. Rev.* **1995**, *95*, 2457.
- S. Yoshikawa, J. Odaira, Y. Kitamura, A. V. Bedekar, T. Furuta, K. Tanaka, *Tetrahedron* **2004**, *60*, 2225.
- A. Ford, E. Sinn, S. Woodward, *J. Chem. Soc., Perkin Trans. 1* **1997**, 927.
- Although the tris(hydroxynaphthyl)benzenes **1** and **4** have low solubility to typical organic solvent such as hexane, ether, chloroform, and dichloromethane, they dissolve in DMSO.
- The reason why compound **1** exists mainly as one conformer with up-up-up form is not clear and now under investigation.
- The ratio of the two conformers of **2** is approximately 2:1 (=up-up-down:up-up-up) at room temperature and 1.2:1 (=up-up-down:up-up-up) at -60 °C.
- The distance between H and O of two different hydroxy groups which are located in the same side is 2.57 Å. This distance is much longer than that between H of OH group and *ipso*-carbon (2.205 Å). Therefore, the compound **1** does not have intramolecular hydrogen bonding between two hydroxy groups.
- a) B. Marciniak, *Acta Crystallogr., Sect. C* **2007**, *63*, o419.

b) R. Parthasarathi, V. Subramanian, N. Sathyamurthy, J. Leszczynski, *J. Phys. Chem. A* **2007**, *111*, 2. c) E. S. Stoyanov, S. P. Hoffmann, K.-C. Kim, F. S. Tham, C. A. Reed, *J. Am. Chem. Soc.* **2005**, *127*, 7664. d) S. J. Grabowski, *J. Phys. Chem. A* **2007**, *111*, 13537. e) S. Maity, G. N. Patwari, *J. Phys. Chem. A* **2009**, *113*, 1760. f) S. Meng, J. Ma, Y. Jiang, *J. Phys. Chem. B* **2007**, *111*, 4128.

12 The fluorescence spectrum of compound **1** given in Figure 3 shows a shoulder. Probably, this shoulder derived from conformers of **1** (OH direction; up–up–up or up–up–down).

13 K. M. Solntsev, P. L. McGrier, C. J. Fahmi, L. M. Tolbert, U. H. F. Bunz, *Org. Lett.* **2008**, *10*, 2429.

14 Phenols are activated as acids by photoirradiation: a) F. D. Lewis, E. M. Crompton, *J. Am. Chem. Soc.* **2003**, *125*, 4044. b) E. M. Crompton, F. D. Lewis, *Photochem. Photobiol. Sci.* **2004**, *3*, 660. However, our system does not include an anion of phenols, because sodium salt of **1** and **9** did not show the same fluorescence with neutral **1** and **9**, respectively.

15 T. Satoh, J. Inoh, Y. Kawamura, Y. Kawamura, M. Miura, M. Nomura, *Bull. Chem. Soc. Jpn.* **1998**, *71*, 2239.

16 The electronic absorption spectra of **9**–**13** are given in Supporting Information.

17 The methoxy-substituted compound **13** does not give the conformationally different stable isomers probably because of steric hindrance of methoxy group with *ana*-hydrogen. It solely exists with methyl group far from *ana*-hydrogen as shown in Table 3.

18 To investigate the S_0 relative stability of **9**-L and **9**-R in DMSO, hybrid DFT calculations including the solvent effect of DMSO by the polarized continuum model (PCM) were performed at the CAM (Coulomb-attenuating method)–B3LYP/6-31G* level with the Gaussian 09 program.¹⁹ These results show that **9**-L is more stable than **9**-R in DMSO as well as in vacuum. Therefore, in this case it is no problem to discuss the absorption/emission maxima in DMSO using the calculated ones in vacuum, which is supported by the fact that the TDDFT (B3LYP) vertical excitation energies calculated in vacuum show good agreement with the experimental absorption/emission maxima in DMSO. The calculated results are given in the Supporting Information.

19 M. J. Frisch, G. W. Trucks, H. B. Schlegel, G. E. Scuseria, M. A. Robb, J. R. Cheeseman, G. Scalmani, V. Barone, B. Mennucci, G. A. Petersson, H. Nakatsuji, M. Caricato, X. Li, H. P. Hratchian, A. F. Izmaylov, J. Bloino, G. Zheng, J. L. Sonnenberg, M. Hada, M. Ehara, K. Toyota, R. Fukuda, J. Hasegawa, M. Ishida, T. Nakajima, Y. Honda, O. Kitao, H. Nakai, T. Vreven, J. A. Montgomery, Jr., J. E. Peralta, F. Ogliaro, M. Bearpark, J. J. Heyd, E. Brothers, K. N. Kudin, V. N. Staroverov, R. Kobayashi, J. Normand, K. Raghavachari, A. Rendell, J. C. Burant, S. S. Iyengar, J. Tomasi, M. Cossi, N. Rega, J. M. Millam, M. Klene, J. E. Knox, J. B. Cross, V. Bakken, C. Adamo, J. Jaramillo, R. Gomperts, R. E. Stratmann, O. Yazyev, A. J. Austin, R. Cammi, C. Pomelli, J. W. Ochterski, R. L. Martin, K. Morokuma, V. G. Zakrzewski, G. A. Voth, P. Salvador, J. J. Dannenberg, S. Dapprich, A. D. Daniels, Ö. Farkas, J. B. Foresman, J. V. Ortiz,

J. Cioslowski, D. J. Fox, *Gaussian 09 (Revision B.01)*, Gaussian, Inc., Wallingford CT, USA, **2009**.

20 Examples wherein the protic hydrogen of an amino group controlled intramolecular charge transfer were reported. In our system, however, charge transfer was not the main reason for the bathochromic shifts in **1** and **9**, judging from NAO atomic charge: a) T. Stalin, N. Rajendiran, *Chem. Phys.* **2006**, *322*, 311. b) P. Dahiya, M. Kumbhakar, D. K. Maity, T. Mukherjee, A. B. R. Tripathi, N. Chattopadhyay, H. Pal, *J. Photochem. Photobiol., A* **2006**, *181*, 338. c) R. V. Pereira, M. H. Gehlen, *Chem. Phys. Lett.* **2006**, *426*, 311.

21 a) C. Niezborala, F. Hache, *J. Am. Chem. Soc.* **2008**, *130*, 12783. b) D. P. Millar, K. B. Eissenthal, *J. Chem. Phys.* **1985**, *83*, 5076. c) R. M. Bowman, K. B. Eissenthal, D. P. Millar, *J. Chem. Phys.* **1988**, *89*, 762. d) Y. Takei, T. Yamaguchi, Y. Osamura, K. Fuke, K. Kaya, *J. Phys. Chem.* **1988**, *92*, 577. e) D. Mank, M. Raytchev, S. Amthor, C. Lambert, T. Fiebig, *Chem. Phys. Lett.* **2003**, *376*, 201.

22 The distances are shown in the Supporting Information.

23 The calculated values of absorption and emission wavelengths are shown in the Supporting Information. HOMO and LUMO at the B3LYP S_0 min and the CIS S_1 min were obtained using the Hartree–Fock (HF) method. We employed the HF orbitals rather than the Kohn–Sham (KS) orbitals for more quantitative orbital analysis, because the HF theory satisfies Koopmans’ theorem while the KS theory does not as long as an approximate exchange–correlation functional is used.

24 The average of wavelengths was estimated based on the Boltzmann distribution of both isomers.

25 The NAO atomic charges of **6**-L and **12**-L are also given in the Supporting Information. We excluded these species in the discussion in Table 4 because they are an unstable conformer compared to the corresponding **6**-R and **12**-R. The compound **6**-R was more stable than **6**-L ($E(L) - E(R) = 1.69 \text{ kcal mol}^{-1}$).

26 The solvent effect of trisubstituted benzene **1**–**5** was investigated. The unsubstituted compound **3** and the methoxy-substituted compounds **2** and **5** showed less solvent effect than **1**, indicating that their excited states are less polarized than that of **1**. The electronic emission spectra are given in the Supporting Information.

27 In the asymmetric unit of **15**, two crystallographically independent molecular structures of **15** were observed.

28 J. A. O’Meara, C. Yoakim, P. R. Bonneau, M. Bös, M. G. Cordingley, R. Déziel, L. Doyon, J. Duan, M. Garneau, I. Guse, S. Landry, E. Malenfant, J. Naud, W. W. Ogilvie, B. Thavonekham, B. Simoneau, *J. Med. Chem.* **2005**, *48*, 5580.; NMR spectrum: J. S. Yadav, B. V. S. Reddy, P. S. R. Reddy, A. K. Basak, A. V. Narsaiah, *Adv. Synth. Catal.* **2004**, *346*, 77.

29 S. Kamila, C. Mukherjee, A. De, *Tetrahedron Lett.* **2001**, *42*, 5955; NMR spectrum: T. K. Macklin, V. Snieckus, *Org. Lett.* **2005**, *7*, 2519.

30 M. J. Plater, *J. Chem. Soc., Perkin Trans. 1* **1997**, 2897.

31 Y. Nishii, Y. Tanabe, *J. Chem. Soc., Perkin Trans. 1* **1997**, 477.